Journal of Electronics, Electromedical Engineering, and Medical Informatics
Multidisciplinary: Rapid Review: Open Access Journal **Vol. 5, No. 2, April 2023, pp: 59-68; eISSN: 2656-8632**

RESEARCH ARTICLE **OPEN ACCESS**

Manuscript received February 10, 2023; revised March 1, 2023; accepted March 12, 2023; date of publication April 3, 2023
Digital Object Identifier (**DOI**): https://doi.org/10.35882/jeemi.v5i2.283

How to cite: N.M.Mary Shindhja and Atul Varshney, "Hybrid βΩ-Indexing Fractal Slotted Multiband Antenna for Electronics Wireless Sensor Applications", Journal of Electronics Electromedical Engineering, and Medical Informatics, vol. 5, no. 2, pp. 59–68, April 2023

Hybrid βΩ-Indexing Fractal Slotted Multiband Antenna for Electronics Wireless Sensor Applications

N.M.Mary Shindhja[1], and Atul Varshney[2]
[1] Department of ECE, Kamaraj College of Engineering & Technology, Madurai, India
[2] ECE Department, FET, Gurukula Kangri (Deemed to be University), Haridwar-249404, Uttarakhand, India

Corresponding author: Atul Varshney (e-mail: atulgkvrightr@ gmail.com)

This work was supported in part by ECE Department, FET, Gurukula Kangri (Deemed to be University), Haridwar-249404, Uttarakhand, India.

ABSTRACT In this proposed work, a compact, low profile, inset-fed βΩ-space-filling curve-based slotted fractal antenna for multi-band wireless applications and narrow-band operations is designed, fabricated, and successfully tested. The measured results of the reflection coefficient and E-plane and H-plane gain radiation patterns are found to be very concord with simulated corresponding results. The antenna resonates at five resonance frequencies 1.91GHz (1.86-1.93GHz), 3.12GHz (3.03-3.21GHz), 5.56GHz (5.50-5.60GHz), 10.75GHz (10.55-11.20GHz) and 13.94GHz (13.72-14.17GHz) with narrow band. Therefore, the proposed antenna is adopted for applications like PCS-1900 (n2 band: 1850-1910MHz), rail mobile radio (1900-1910MHz), DCS-IMT gap (n98/n39 band: 1880-1920MHz), WCDMA (1900MHz), X-band (10.55-11.20GHz) and Ku-band (13.72-14.17GHz) applications. The antenna parameters gain, directivity, and efficiency are greatly improved by the 50% reduction in ground length. Good impedance matching is achieved by the use of inset feeding with a 50Ω port at an operating frequency of 3.1GHz. The antenna exhibits 2.94dBi gain at the operating frequency. A new hybrid βΩ- space-filling curve has been utilized for the slotted fractal proposed antenna design. The antenna is fabricated on an FR4 substrate with compact dimensions (39.05mm x 32.25mm x 1.6mm) at a frequency of 3.1GHz.

INDEX TERMS Beta Omega (βΩ) space-filling curve, Fractal antenna, Hilbert curve, Inset-fed, Multiband, Wireless sensor applications.

I. INTRODUCTION

Microstrip antennas are low-profile antennas where the metal patch mounted at a ground level with a dielectric material in-between constitutes a microstrip or patch antenna. These become so popular because of the multiple frequency bands used for wireless applications. The shorting plate is used along with a meander-type radiation patch to minimize the size of the antenna. The meandering in the patch leads to a large reduction in the required dimensions of the patch for various band operations. Instead of a rectangular patch, the βΩ-space filling curve is used for multi-band planar antennas for mobile radio applications.

In the past decades, the microstrip patch antenna has drawn the attention of several researchers due to its feasibility and size reduction. This leads to the development of microstrip patch antennas in different fields such as radar, aircraft, satellite communication, biomedical applications, Microstrip to Waveguide Transitions as sensors, and wireless communications in MIMO, Massive MIMO, Super-massive MIMO, beam forming, and phased array antennas [1-11]. The performance of the microstrip antenna depends on size, resonant frequency, operating band, -10dB- impedance fractional bandwidth (FBW), Gain, radiation pattern, radiation efficiency, and overall dimension of the substrate [12]. In the microstrip patch antenna, the most widely used shapes of the patch are circular, square, rectangular, elliptical, ring triangular, etc. The different shapes of the antenna helps in the compactness and miniaturization of antenna size [13]. For

wireless recent advanced applications, some other types of slot antennas are designed and developed.

Fath Elrahman *et al.*, have designed and investigated a U-slot antenna for dual-band applications to achieve wider bandwidth and high gain of 6.2 dB at 2.4GHz and 5.0438 dB at 4.6 GHz [14]. The L-shaped corner slots are used at diagonally opposite corners to achieve compactness for circular polarization (CP) operation with an axial ratio of 3dB bandwidth and 6.4 dBi gain at a frequency of 8.1GHz [15]. S. Thakur *et al.*, have presented a low profile, two L-shaped slotted rectangular patch antennae for C-band satellite applications [16]. R. Ahmed and Md. F. Islam have been presented with an electrically small W-slotted multiband microstrip antenna for wireless communication systems, especially for military spectrum (X band). Resonant frequencies occur in C, X, and Ku bands with an average gain of 4.5 dBi [17]. The novelties in the structure of the patch were reported in the literature [18, 19, and 20]. Recently researchers have shown much interest in developing fractal-shaped patch antennas because the fractals have two common properties: space-filling and self-similarity which help to achieve wide and multiband antennas with reduced size [21, 22]. Initially, these geometries were used to construct monopole and loop antennas which came into existence during the 1990s [23, 24]. The size of the ground plane in the fractal antenna influences the antenna to work at different frequencies [25, 26]. The planar monopole antenna is designed using CPW feed to achieve ultra-wide bandwidth [27]. The basic geometries used for fractal antennas are Sierpinski gasket, Minkowski Island, Sierpinski carpet, Koch Snowflake, and Hilbert. The Hilbert curve slot is used to design the antenna where four times bandwidth enhancement is obtained by increasing the number of iterations at the frequency of 2.4GHz [28, 29].

In the literature, it is clear that the researcher developed the design by introducing the simple slots or single/dual combinations of Minkowski, Koch, etc curves and their replications. In this work, a hybrid slot is applied within the patch to achieve multiband behavior. The work is important as it is designed to cover the complete microwave band from L-band to Ku-band functioning. The proposed antenna is designed for penta-narrow band antenna based on the new hybrid fractal slots for various wireless PCS, wireless rail mobile, Sub-6GHz, Wi-Fi5, X-band, and Ku-bands applications. The main aim of this work is to design an antenna using space-filling techniques that can be tuned from lower frequencies to higher frequencies without external fractals. Another objective of this work is to design a slotted antenna based on fractal geometrical combinations. The proposed slotted fractal antenna is based on Beta Omega (βΩ) space-filling curve [30]. The article sub-sections describe the antenna design analysis at operating frequency 3.1GHz, its development, fabrication, and measurements. The proposed antenna is developed in three iterations which have U-shaped geometry and are derived from the way the curve passes the quadrant of size 4X4.

II. ANTENNA DESIGN

Initially, a line segment of length "L" is available as shown in FIGURE 1(a). Then it is bent into three equal parts by dividing the length L by 3. Thus, each side length of the U-shape curve is formed. The Ω-shape curve is formed by bending the two corner (3rd and 4th quadrant) arms of the U-shape again in U-shape with each side length dimension equal to ((L/3)/3) i.e., L/9. Ω-shape is further bent with side length L/9 at the middle of the 1st and 2nd quadrants to form a Hilbert curve. The β-shape curve is also the result of the bending of the U-shaped curve in four folds as shown in FIGURE 1(b) with the same L/9 length side dimension in all four quadrants.

The basic fractal elements are shown in FIGURE 1(a). Primarily these include line segments, U-shaped curves, Ω-shaped curves, Hilbert curves, β-shaped curves, etc. The basic geometry generations of β-shaped and Ω-shaped curves from U-shaped curves are shown in FIGURE 1(b). The red color circle represents the initial and termination of points and the black color dots represent the movement of the line segment direction.

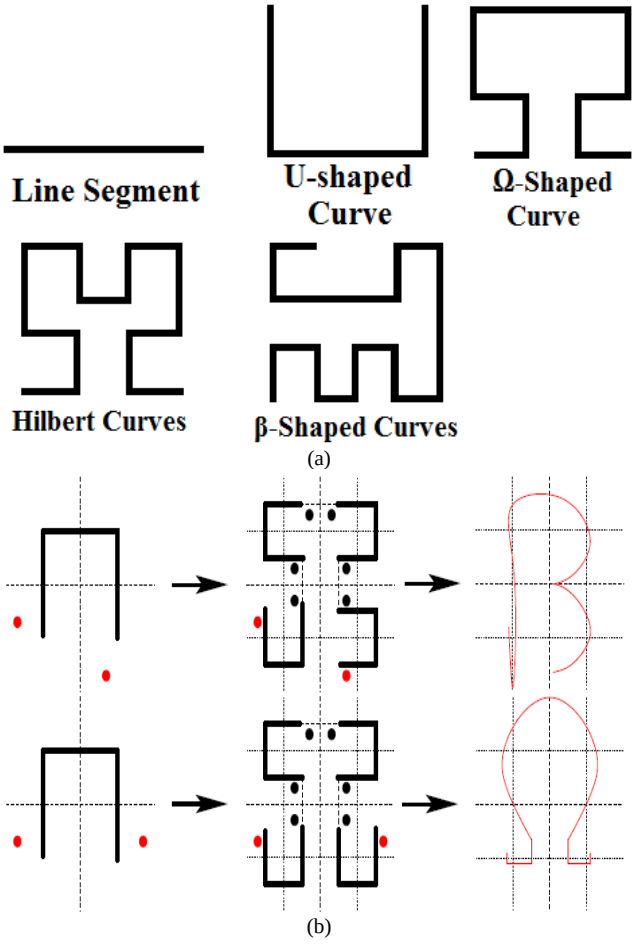

FIGURE1. **(a) Fundamental Fractal curves (b) Fundamental β and Ω-curves Generator**

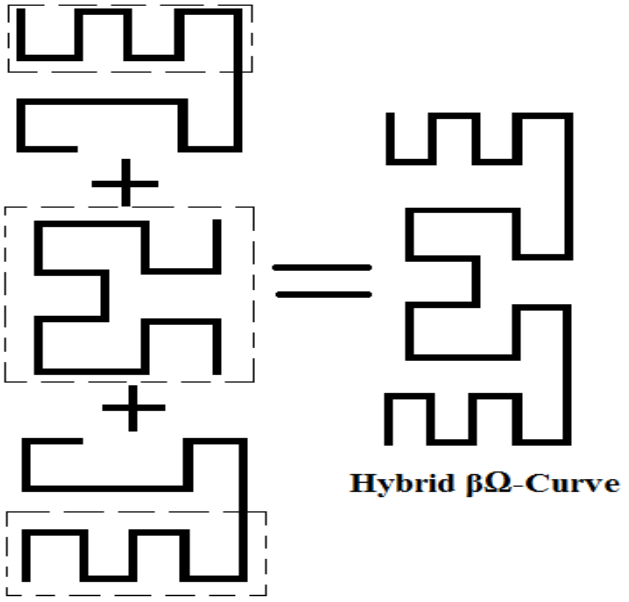

FIGURE2. **The basic unit of Hybrid βΩ space-filling curves**

The proposed antenna geometry is developed from the hybrid combination of the basic unit of β-shape and Ω shape combination curves as shown in FIGURE 2 [30, 33]. The dash box curves are added together to form the basic unit of hybrid βΩ-space filling curves. That is not exactly but it is much closer to Hilbert curves space-filling fractal geometry [30, 33].

A. ANTENNA GEOMETRY AND DIMENSIONS

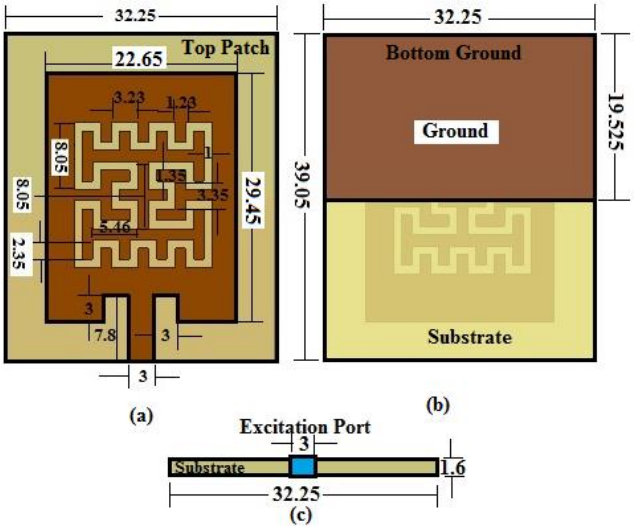

FIGURE3. **Antenna Geometry with all dimensions (in mm) (a) Front View (b) Bottom view and (c) Antenna Excitation Port**

The proposed antenna is designed on an FR4 substrate having a relative permittivity of 4.4 and a thickness of 1.6mm. The overall size of the antenna is $0.4035\lambda_0 \times 0.33325\lambda_0$ (39.05mm × 32.25mm). The antenna is designed at a frequency of 3.1GHz. The length and width of the rectangular patch are computed with the standard design equations [12, 29]. The basic unit of hybrid βΩ-space filling curves is a mirror image across the vertical axis, then added together and finally subtracted from the standard rectangular patch (32.25mm X 39.05mm) to get the desired slotted fractal geometry. The proposed slotted fractal antenna patch and ground design geometries are shown in FIGURE 3 (a-b) with all dimensions. All dimensions are measured in mm. The RF excitation source position is shown in FIGURE 3 (c).

III. ANTENNA DESIGN DEVELOPMENT AND OPTIMIZATION

A. HYBRID BΩ SPACE-FILLING FRACTAL ANTENNA DESIGN DEVELOPMENT

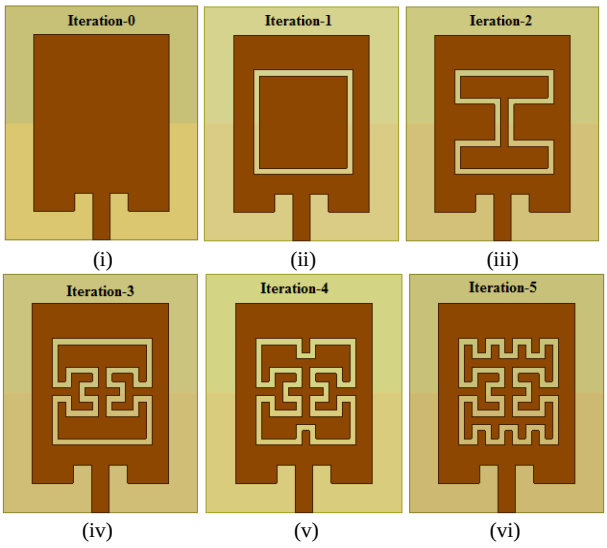

FIGURE4. **Iterations of patch development of βΩ-fractal antenna**

The antenna design development from a basic rectangular patch antenna at operating frequency 3.1GHz (Iteration 0) to iteration 5 are shown in FIGURE 4. All the five iteration steps from iteration 1 to iteration 5 of βΩ-indexing based space-filling fractal slotted antenna on a basic rectangular patch of iteration 0 are displayed in FIGURE 5 and their corresponding reflection coefficient plots are also represented as comparative study cases with 50% reduced ground length i.e., 19.525mm. It is noticed that in all cases the behavior of the slotted fractal antenna is multi-narrow band type. The comparisons of all iterations in terms of simulated antenna parameters are depicted in Table I. It is observed that as the slotted fractal in the rectangular patch of iteration becomes dense with βΩ-curves, the antenna peak gain and maximum radiation efficiency of the antenna becomes down from 81.18% (iteration1) to 57.23% (iteration5) at operating frequency 3.1GHz. The final βΩ-indexed space-filling fractal slotted antenna resonates at five different resonance frequencies with narrow bandwidths 1.91GHz (1.86-1.93GHz), 3.12GHz (3.03-3.21GHz), 5.56GHz (5.50-5.60GHz), 10.75GHz (10.55-11.20GHz) and 13.94GHz (13.72-14.17GHz).

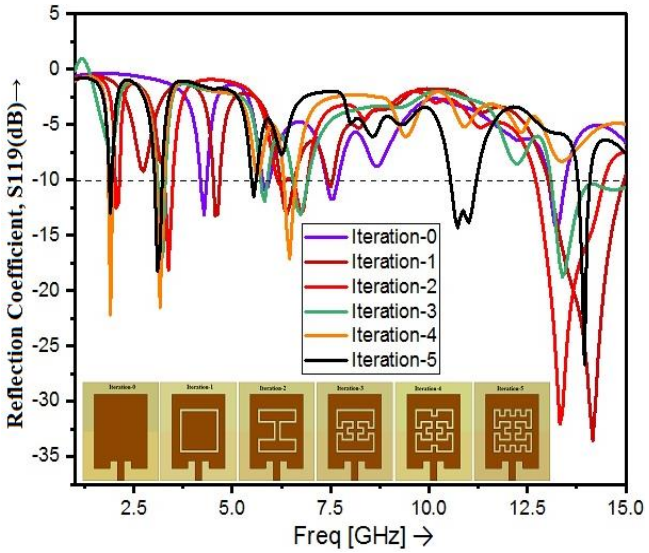

FIGURE 5. **Effect of intermediate space filling iterations**

TABLE 1
Effect of intermediate space filling iterations

I	N	f_r (GHz)	BW (GHz)	G (dBi) at f_0	D (dBi) at f_0	η at f_0 (%)
0	04	4.31 5.86 7.55 13.28	4.20-4.35 5.78-5.95 7.39-7.69 13.03-13.47	4.45	5.96	70.6
1	04	4.57 6.37 7.48 14.15	4.52-4.69 6.22-6.58 7.42-7.55 13.03-14.96	3.72	4.628	81.18
2	04	2.08 3.40 6.78 13.34	2.03-2.14 3.27-3.50 6.10-6.91 12.71-14.45	4.25	5.65	72.46
3	04	3.26 5.82 6.76 13.42	3.11-3.30 5.73-5.90 6.54-6.93 13.10-15.12	3.68	5.56	64.96
4	03	1.93 3.18 6.48	1.86-1.97 3.07-3.27 6.31-6.62	3.45	5.522	62.13
5	05	1.91 3.12 5.56 10.75 13.94	1.86-1.93 3.03-3.21 5.50-5.60 10.55-11.20 13.72-14.17	2.94	5.36	57.23

***I= Iteration no., N=no. of Bands, f_r=resonance frequency, BW=-10dB Bandwidth, G=Gain, D=Directivity, η=radiation efficiency, f_0=Design Frequency**

B. GROUND LENGTH OPTIMIZATION

The effect of ground length with a 100% length of 39.05mm and 50% reduced length of 19.525mm are displayed in terms of their simulated antenna parameters in Table II and their corresponding reflection coefficients S_{11} plots are displayed in FIGURE 6. It is observed that the effect of a 50% reduction in ground length is that the radiation efficiency is greatly improved from 2.67% to 57.23%. The main purpose of the reduction of ground length is to improve the gain and directivity values. Finally, the gain and directivity become positive and highly improved with reduced ground length.

TABLE 2
Ground Length Variation

Ground length (mm)	N	f_r (GHz)	BW (GHz)	G (dBi) at f_0	D (dBi) at f_0	η at f_0 (%)
39.05 (100%)	06	1.72 3.04 5.28 5.92 10.76 13.23	1.65-1.80 2.96-3.08 5.16-5.32 5.75-6.01 10.55-11.13 13.09-13.27	-16.1	-0.34	2.67
19.525 (50%)	05	1.91 3.12 5.56 10.75 13.94	1.86-1.93 3.03-3.21 5.50-5.60 10.55-11.20 13.72-14.17	2.94	5.36	57.23

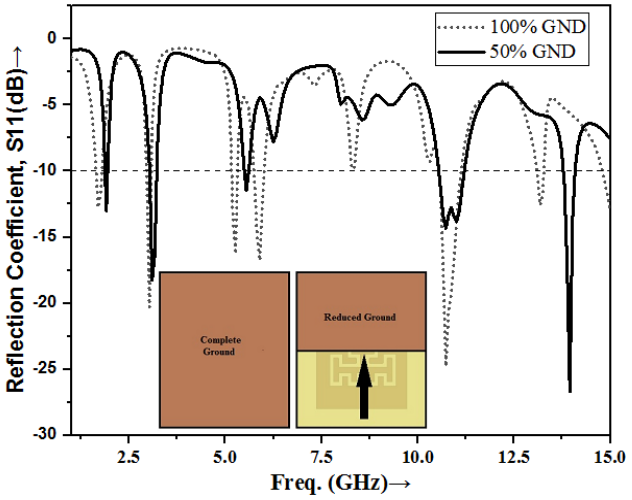

FIGURE6. **Effect of ground length variation**

C. EFFECT OF INSET FEED

The main purpose of feeding techniques is to achieve better impedance matching. Initially, the antenna is edge-fed with a 50Ω feed line length of 4.8mm and a feed line width of 3 mm. It will resonate at six resonant frequencies 3.05GHz, 5.50GHz, 8.5 and 9.97GHz, 12.15GHz and 13.97 GHz below -10dB reflection coefficient values within four narrow and one wideband (8.16-10.7GHz). The inset-fed antenna resonates at five resonant frequencies within five narrow bands below -10dB S_{11} values as displayed in FIGURE 7 and represented in Table III. It is noticed from Table that the antenna parameters gain, directivity, and radiation efficiency are decreased by a very tiny amount nevertheless not much advantage in terms of antenna parameters has been observed by inset feeding except that space-filling area and better impedance matching at design frequency 3.1GHz. The antenna impedance in inset feed is (50.69-j4.50) Ω and that in the case of edge feed is (37.04-j1.03) Ω at 3.12GHz. In inset feeding the antenna impedance is closer to 50 Ω port impedance and therefore high impedance matching is achieved with inset feed. Because of

that in the proposed design inset feeding is the best suitable choice.

TABLE 3
Effect of Feed Position

Feed length (mm)	Bands	f_r (GHz)	-10 dB BW (GHz)	G (dBi) at f_0	D (dBi) at f_0	η at f_0 (%)
4.8 (Edge feed)	05	3.05 5.50 8.5,9.97 12.15 13.97	2.97-3.15 5.42-5.57 8.16-10.7 11.87-12.32 13.78-14.19	3.077	5.49	57.35
7.8 (Inset feed)	05	1.91 3.12 5.56 10.75 13.94	1.86-1.93 3.03-3.21 5.50-5.60 10.55-11.20 13.72-14.17	2.94	5.36	57.23

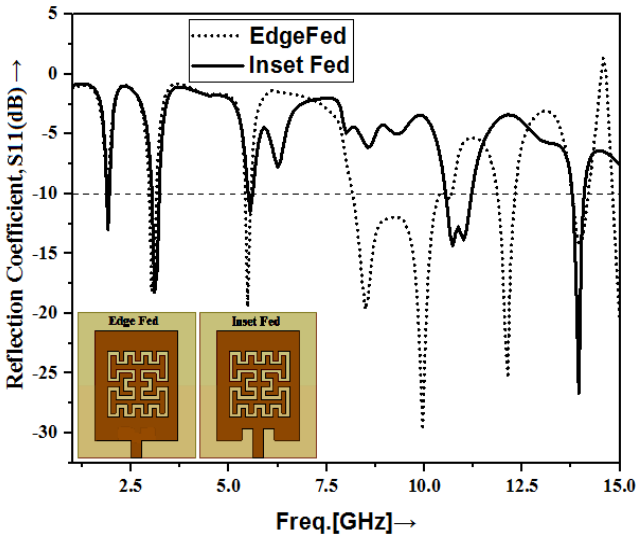

FIGURE7. **Effect of feed line (a) Edge feed (b) Inset feed**

IV. ANTENNA PROTOTYPE

The hybrid βΩ-space filling fractal antenna prototype is fabricated using a photolithography process and chemical etching technology. The front views of the carpet-like patch structure and 50% reduced ground bottom view with a 50Ω connector soldered for excitation of microwave RF signal are depicted in FIGURE 8. This may introduce some compulsory fabrication and soldering losses.

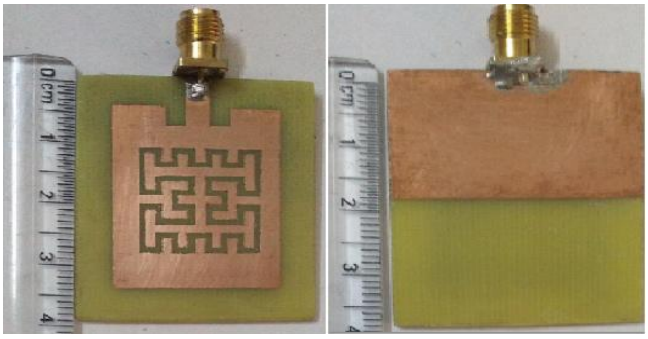

(a) (b)

FIGURE 8. **Prototype of Antenna Top and Bottom view**

V. RESULTS

The fabricated hybrid βΩ-space filling fractal antenna is experimentally verified with the measurement in the laboratory through a vector network analyzer (VNA: Agilent N5247A) and Electric and Magnetic radiation patterns are measured in an anechoic chamber using 10° step rotation of steppers motor. The reflection coefficient, S_{11} on VNA, and radiation pattern and gain measurement setup in an anechoic chamber are depicted in FIGURE 9.

(a) (b)

FIGURE 9. **Measurement setup (a) reflection coefficient, S11 on VNA (left) (b) Gain measurement in an anechoic chamber (right)**

A. REFLECTION COEFFICIENTS (S_{11})

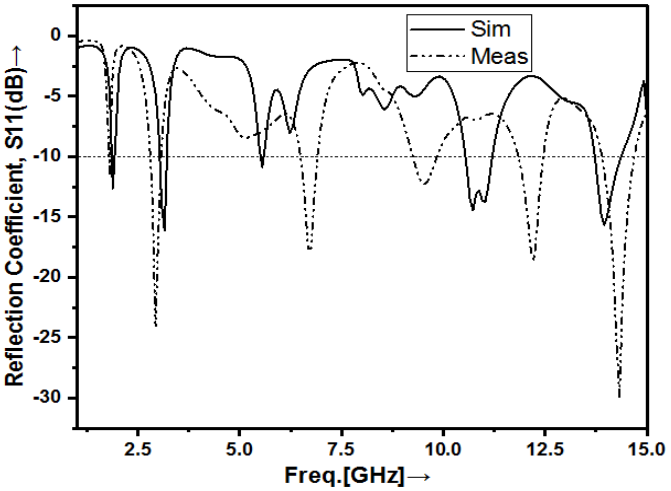

FIGURE 10. **Measured and simulated Reflection Coefficient Curves**

The simulated and measured reflection coefficient curves are observed and plotted on the same curve as displayed in FIGURE 10. The four narrow band reflection coefficients are observed below -10dB in the simulated reflection coefficient curve at resonance frequencies 1.91 GHz (1.86-1.93 GHz), 3.12 GHz (3.03-3.21 GHz), 10.75 GHz (10.55-11.20 GHz) and 13.94 GHz (13.72-14.17 GHz). It is observed that both measured and simulated reflection coefficients are identical at first, second, and fourth resonance frequencies with very tiny shifts in resonance frequencies. At the second resonance frequency of 3.12GHz in the simulated S_{11} plot, two shifted new frequency bands at

9.528 GHz (9.22-9.82 GHz) and 12.22 GHz (11.85-12.45 GHz) have been observed in the measured S_{11} plot, and one additional resonance is observed at resonance frequency 6.68 GHz (6.45-6.90 GHz). This deficiency in multi-narrowband behavior between measured and simulated reflection coefficient curves is because of the soldering, fabrication, and measuring equipment errors.

B. RADIATION PATTERNS

The E-plane and H-plane radiation patterns are measured in an anechoic chamber using a reference horn antenna with a step size of 10° rotation at four resonance frequencies 1.91 GHz, 3.1 GHz, 10.75 GHz, and 13.94 GHz. Both radiation patterns in E-plane and H-plane patterns are found in concord. It is noticed that the radiations of the antenna are maximum in normal to its patch and ground surfaces at all four resonant frequencies. The simulated and measured E-plane and H-plane gain radiation patterns are represented in FIGURE 11.

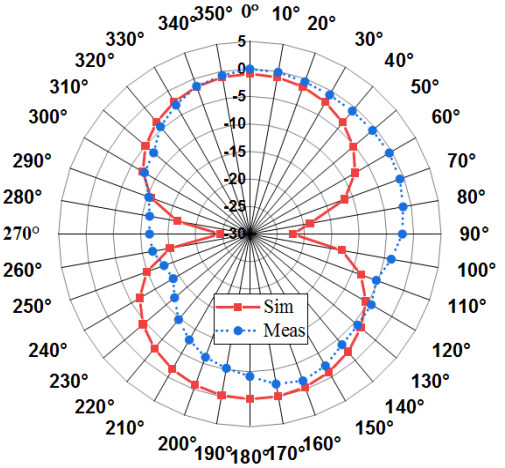

(a)E-Plane @1.91GHz

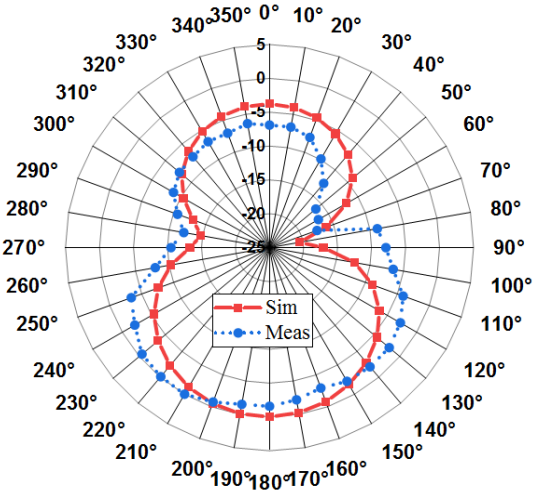

(b)E-Plane @3.1GHz

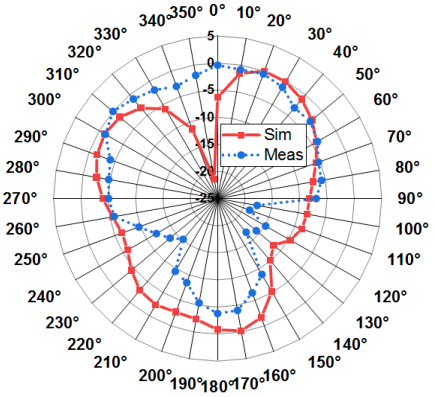

(c)E-Plane @10.75GHz

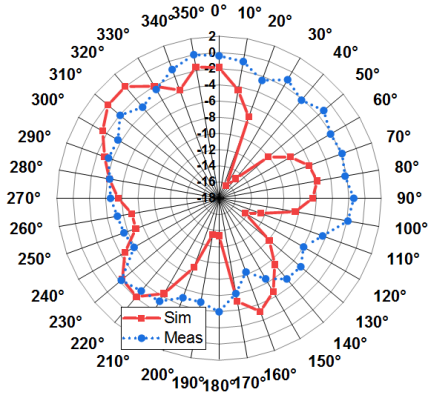

(d)E-Plane @13.94GHz

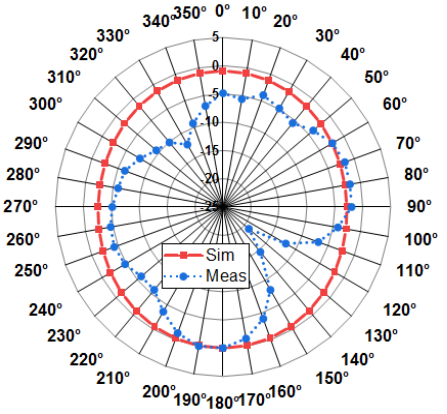

(e)H-Plane @1.91GHz

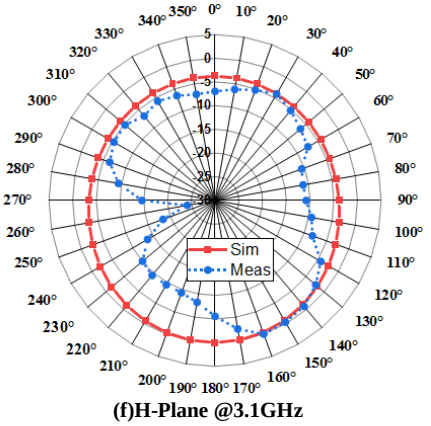

(f)H-Plane @3.1GHz

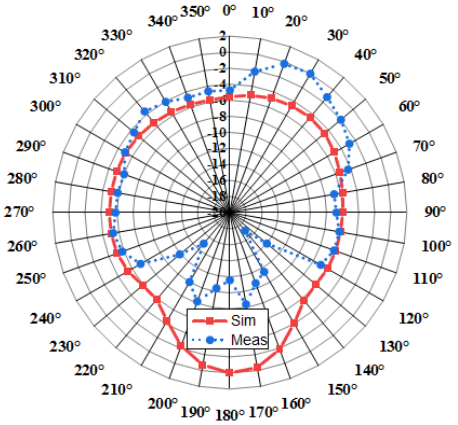

(g)H-Plane @10.75GHz

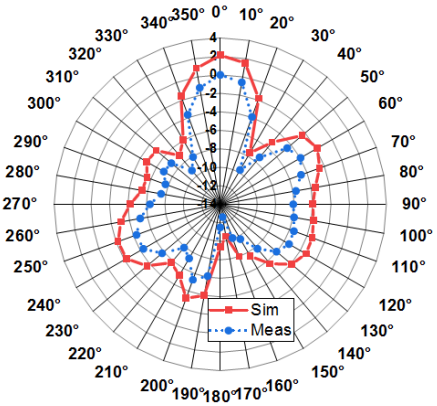

(h)H-Plane @13.94GHz

FIGURE11. **E-plane and H-Plane Radiation Patterns of the antenna at four resonance frequencies**

C. GAIN PLOT

As the 3D-radiation pattern of the βΩ-curve slotted fractal antenna is Omni-directional at the design frequency, the dBi gain plot against the frequency sweep from 1.5GHz to 15 GHz is plotted as represented in FIGURE 12. The gain is found positive over the full frequency span. At five resonance frequencies, the gain is found 0.5dBi, 4.32dBi, 14.9dBi, 22.49dBi, and 4.51dBi respectively.

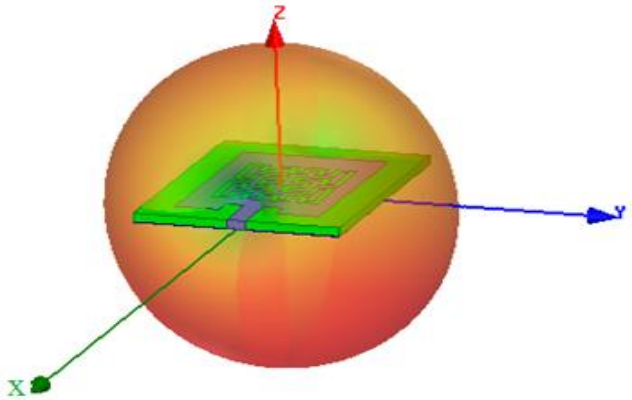

(a)

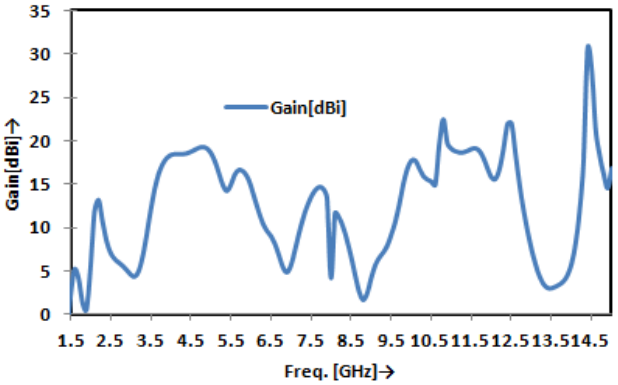

(b)

FIGURE 12. **(a) 3D-radiation pattern (left) and (b) Gain plot of the βΩ-fractal antenna (right)**

VI. DISCUSSION

The proposed Hybrid Beta omega (βΩ) curve fractal antenna is economical as it is fabricated on a low-cost FR-4 substrate and compact with a size of 32.2 mm × 39.05mm. It exhibits five narrow bands in microwave 1 GHz to 15 GHz frequency band with five resonant frequencies. It exhibits an omnidirectional radiation pattern in the H-Plane and a Figure of Eight-like structure in the E-Plane. The antenna is an excellent candidate where high gain is desired. Since it exhibits the highest gain as compared to literature existing antennas. A gain of 16.2 dBi at a frequency of 5.56 GHz and a gain of 21.1 dBi at a frequency of 10.75 GHz. It exhibits an excellent impedance match at the designed frequency of 3.1 GHz. As the bottom side has reduced ground more numbers of passive components can be added to this surface. This antenna can easily be converted into a frequency/ pattern/ polarization reconfigurable antenna by just adding a few numbers of switching PIN/varactor diodes at suitable locations.

The main weakness of the proposed antenna is that the structure looks as complex as a snake shape of a continuous combination of the beta-omega space-filling slot to increase the electrical length of the simple patch. Another limitation of this work is that the connectorsoldered is of the value up to 6 GHz therefore the measured results are in excellent matched with the simulated results up to this frequency range. Beyond 6 GHz the measured results show shifting of the higher bands from 6 GHz to 15 GHz. This problem could be resolved by the use of the correct 15 GHz SMA connector.

L. Singh and M. Kaur have reviewed several kinds of fractal antennae and compared their resultant parameters [28]. The proposed work is compared with the previously existing similar antennas in terms of their performance parameters like type of curve used for fractal, antenna size, number of bands and their nature, resonance frequency, bandwidth, and gain. These results are tabulated in Table IV. Sierpinski Gasket Fractal has the minimum size for only dual bands and good gain nevertheless proposed antenna is tuned for penta-narrow bands with little large antenna size with excellent gain and stable radiation characteristics. It has been observed from the

comparison of previous similar antennas table that the proposed antenna has the smallest antenna size, and highest gain as compared to all existing reference antennas [27,29,31,32,]. The present antenna possesses the five-resonance band. All five bands have narrow bandwidths (TABLE 4).

TABLE 4

Comparison of Proposed Antenna with the Previously Similar Existing Antennas

Ref.	Used Curve Type	Ant. Size (LxW) (in mm^2)	Band	f_r (GHz)	BW (GHz)	G (dBi)
[34] 2016	H-tree fractal Geometry	55 x 50	single Wide Band Dual Tuned	3.0 & 5.2	1.5-6.32	5.18
[35] 2015	Sierpinski Gasket Fractal	17.89 x 21.45	Dual Narrow-band	5.51 9.65	5.4-5.71 9.4-9.82	5.918 11.83
[36] 2016	Hexagonal patch	45 x 44.92	Quad-narrowband	3.55 5.94 8.50 9.47	3.57-3.58 5.9-6.05 8.41-8.59 9.2-10.50	4.25 5.05 5.77 8.55
[37] 2016	Triangular fractal techniques	NA	Multi-narrow band	3.0 4.8 5.24 8.1 8.6 9.07	Narrow bands	----- ----- 7.39 8.26 ----- 9.74
[38] 2016	Half rectangular fractal	40×30	Quad narrow band	3.25 4.04 5.34 6.02	3.19-3.29 3.98-4.09 5.4-5.46 5.97-6.06	4.27 6.487 9.94 5.062
[29] 2018	Koch-Minkowski slot Koch-Koch slot	38.92×45	Dual tune wide band	2.41&8.34 2.68&8.38	6.67-10 6.76-10	7.88 8.30 3.72 7.77
[27] 2013	Four iterative Concentric Nano-arm fractal antenna	63.5×65	Multi tuned Ultra-Wide band	2.875, 5.45 8.05 10.35	2.55-11.84	5
[31] 2021	Tri-arms fan-shaped (outer fractal)	66.4x66.4	Dual narrow band	1.68 2.5	1.62-1.73 1.81-3.0	4.08
[32] 2022	Dodecagon -shaped tri delta loaded (outer fractal) transformer fed	52×59	Tri-wide band	3.1 5.6& 8.98 10.94	1.79–3.73 5.27–6.10 6.48-11.47	4.12
This work	Hybrid Beta omega (βΩ) curve	32.2 × 39.05	Penta narrow band	1.91 3.12 5.56 10.75 13.94	1.86-1.93 3.03-3.21 5.50-5.60 10.55-11.20 13.72-14.17	0.5 4.32 16.2 21.1 4.91

VIII. CONCLUSION

The gain of the simulated antenna is 4.32 dBi at 3.1GHz and 4.91 dBi at 13.94GHz. The Proposed multi-band antenna exhibits stable gain radiation characteristics in the E-plane and H-plane and also provides a good reflection coefficient at five resonant frequencies within the specified frequency sweep from 1 GHz to 15 GHz. All five bands have narrow -10 dB impedance fractional bandwidths 3.68% (1.86-1.93GHz), 5.8% (3.03-3.21 GHz), 1.83% (5.50-5.60 GHz), 6.04% (10.55-11.20 GHz) and 3.23% (13.72-14.17 GHz). Therefore, the antenna is the best suitable choice for GSM, WCDMA, mobile radio (1.86-1.93 GHz), Maritime, Radar (3.03-3.21 GHz), Wi-MAX (5.50-5.60 GHz), Radio Location and ITU band applications (10.55-11.20 GHz), and aircraft, spacecraft, satellite-based communication systems (13.72-14.17 GHz). The variation in the fabricated results from the simulated results can be minimized by proper soldering, careful fabrication, and measurement. In the future, the antenna can be converted into frequency reconfigurable by using PIN/varactor diodes and bandwidth and gain can be enhanced by the use of metamaterial SRR, superstrate, EBG, and PBG structures.

ACKNOWLEDGMENT

The authors are grateful to Hon'ble Vice-Chancellor, Gurukul Kangri (Deemed to be University), Haridwar, India for providing hardware, Software, and technical support in various measurements, respectively for the development of the project.

REFERENCES

[1] A. Varshney, V. Sharma, "A Comparative Study of Microwave Rectangular Waveguide-to-Microstrip Line Transition for Milli-meterwave, Wireless Communications and Radar Applications," *Microwave Review*, Vol.26, no.2, pp. 26-37, Dec. 2020.

[2] A. Varshney, V. Sharma, C, Nayak, A. K. Goyal, Y. Massoud, "A Low-Loss Impedance Transformer-Less Fish-Tail-Shaped MS-to-WG Transition for K-/Ka-/Q-/U-Band Applications," *Electronics*, Vol. 12, no. 3, 670, Jan. 2023. DOI: 10.3390/electronics12030670.

[3] A. Varshney, V. Sharma,I. Elfergani, C. Zebiri, Z. Vujicic, J. Rodriguez. 2022. "An Inline V-Band WR-15 Transition Using Antipodal Dipole Antenna as RF Energy Launcher @ 60 GHz for Satellite Applications." *Electronics*, Vol. 11, no. 23: 3860, pp. 1-16, Dec. 2022. DOI: 10.3390/electronics11233860.

[4] A.Varshney, V. Sharma, T.M. Neebha, R. Kumar, "A compact low-cost impedance transformer-fed wideband monopole antenna for Wi-MAX N78-band and wireless applications," *Microstrip Antennas, Book Chapter*, CRC Press, Taylor and Francis, 1st ed., Nov, 2022. DOI: 10.1201/9781003347057-20.

[5] D. K. Janapala, M. Nesasudha, M. Neebha, et al., "Design and Development of Flexible PDMS Antenna for UWB-WBAN Applications," *Wireless Personal Communications*, Vol. 122, no.5, Feb. 2022. DOI: 10.1007/s11277-021-09095-7.

[6] J. Kulkarni, C.Y. D. Sim, A. Desai, et al., "A Compact Four Port Ground-Coupled CPWG-Fed MIMO Antenna for Wireless Applications," ARABIAN JOURNAL FOR SCIENCE AND ENGINEERING, Vol. 47, no. 1, pp. Feb. 2022. DOI: 10.1007/s13369-022-06620-z.

[7] J. Kulkarni, A. G. Alharbi, A. Desai, C. Y. D. Sim, "Design and Analysis of Wideband Flexible Self-Isolating MIMO Antennas for Sub-6 GHz 5G and WLAN Smartphone Terminals," *Electronics*, Vol. 10, no. 23, pp. 1-21, Dec 2021. DOI: 10.3390/electronics10233031

[8] Jinling Zhang, Chen Han, Zhanqi Zheng, Xiongzhi Zhu, Xiaohui Li, "A Fast and Efficient Beamforming Algorithm Imitating Plant Growth Gene for Phased Array Antenna," Hindawi, Vol. 2022, Article ID 6987814, 9 pages, Nov. 2022. DOI:10.1155/2022/6987814.

[9] E. G. Larsson, O. Edfors, F. Tufvesson and T. L. Marzetta, "Massive MIMO for next generation wireless systems," in IEEE

Communications Magazine, vol. 52, no. 2, pp. 186-195, Feb. 2014. DOI: 10.1109/MCOM.2014.6736761.
[10] J. Wu, "Research on Massive MIMO Key Technology in 5G," IOP Conf. Series: *Materials Science and Engineering*, 466, 012083, 2018. DOI:10.1088/1757-899X/466/1/012083.
[11] Tun HM, Lin ZT, Pradhan D, Sahu PK. Slotted Design of Rectangular Single/Dual Feed Planar Microstrip Patch Antenna for SISO and MIMO System. In2021 International Conference on Electrical, Computer and Energy Technologies (ICECET) 2021 Dec 9 (pp. 1-6). IEEE. DOI: 10.1109/ICECET52533.2021.9698738.
[12] C. A. Balanis, *Antenna Theory Analysis and Design*. 2nd ed. USA: JohnWiley and Sons, reprints 2009.
[13] V. G. Kasabegoudar, "Analysis of Coplanar Capacitive Coupled Wideband Microstrip Antennas," *Inter J of Engg Trends and Tech (IJETT)*, Vol. 69, no. 9, pp. 45-50, Sep. 2021.DOI: 10.14445/22315381/IJETT-V69I9P206.
[14] F. Elrahman, I. Khalifa , A. A. Ibrahim , M. Z. Ibrahim, M. M. Fathalrahman , M. A. Alhassan, "Design of Dual-Band Microstrip Antenna with U-shaped slot," *Inter J of Engg Trends and Tech (IJETT)*, Vol. 58, no. 1, Jan. 2018. DOI: 10.14445/22315381/ijett-v55p208.
[15] M. A. El-Hassan, K. F. A. Hussein, K. H. Awadalla, "A Novel Microstrip Antenna with L-Shaped Slots for Circularly Polarized Satellite Applications," *IET Jornal*, Vol. 2019, no. 12, pp. 8428-843, Aug. 2019. DOI: 10.1049/joe.2019.0921.
[16] S. Thakur, R. K. Vishwakarma , R. Gurjar, "A Double L-shaped Slot Loaded Microstrip Antenna for Wideband," *Inter J on Comm (IJC)*, Vol. 3, Mar. 2014.
[17] R. Ahmed, Md. F. Islam, "W-Shaped slot Microstrip Patch Antenna for Multiband Applications," *Inter J of Engg Trends and Tech (IJETT)*, Vol. 26, no. 5, pp. 282-285, Aug. 2015.DOI:10.14445/22315381/IJETT-V26P249.
[18] W. Ren, Z. Shi,Y. Li,and K. Chen, (2006) "Compact Dual-Band T-Slot Antenna for 2.4/5 GHz Wireless Applications," *Communications, Circuits and Systems Proceedings, IEEE*, Vol. 4, pp. 2493-2497, July 2006. DOI: 10.1109/ICCCAS.2006.285181.
[19] A. M. Abbosh , "Miniaturized Microstrip-Fed Tapered-Slot Antenna With Ultra-wideband Performance," *IEEE Antennas And Wireless Propagation Letters*, Vol. 8, pp. 690-692, July 2009. DOI: 10.1109/LAWP.2009.2025613.
[20] A.A. Eldek, A. Z. Elsherbeni, and C. E. Smith, "Square slot antenna for dual wideband wireless communication systems," *J of Electromag Waves and App (JEMWA)*, Vol. 19, no. 12, pp. 1571-1581, April 2012. DOI: 10.1163/156939305775537366.
[21] C. Pucnte, J. Romeu, R. Pous and A. Cardma, "On the Behavior of the Sierpinski Multiband Fractal Antenna," *IEEE Truns Anfemas* Propagut, Vol. 46, no.4 , pp 517-524, April 1998. DOI: 10.1109/8.664115.
[22] P.E. Mayes, "Frequency-Independent antenna and broad-band derivatives thereof," Proc. *Of the IEEE*, Vol. 80, no.1, pp. 103-112, Jan l992. DOI: 10.1109/5.119570.
[23] N. Cohen and R. G. Hohlfed, "Fractal Loops and The Small Loop Approximation," *Coilinruncialions Quarterly*, pp 77-78 I , wintcr 1996.
[24] C. Puente, J. Romeu, R. Pous, J. Ramis and A. Hijazo, "Small but long Koch fractal monopole," *Electronics Letters*, Vol. 34, no.1, pp. 9-10, Jan. 1998. DOI: 10.1049/el19980114.
[25] A. Jamil, M. Z. Yusoff, N. Yahya, M. A. Zakariya, "A compact multiband hybrid Meander-Koch fractal antenna for WLAN USB dongle," *IEEE Conference on Open Systems (ICOS2011)*, pp. 290–293, Sep. 2011. DOI: 10.1109/ICOS.2011.6079295.
[26] J.P. Jacobs, "Efficient resonant frequency modeling for dual-band Microstrip monopole antennas by Gaussian process regression," *IEEE Antenna Wirel Propag Lett*, Vol. 14, pp. 337–341, 2014. DOI: 10.1109/LAWP.2014.2362937.
[27] R. Kumar and S. Gaikwad, "On the Design of Nano-arm Fractal Antenna for UWB Wireless Applications," *J of Microw, Optoelectr and Electromag App*, Vol. 12, no. 1, June 2013. DOI: 10.1590/S2179-10742013000100013.
[28] L. Singh, M. Kaur, "Review of Microstrip Patch Antenna using Fractal Techniques for Wireless Applications," *Inter J of Engg Trends and Tech (IJETT)*, Vol. 49, no. 6, pp. 409-413 July 2017. DOI: 10.14445/22315381/IJETT-V49P263.
[29] N. Sharma, V. Sharma, "A design of Microstrip Patch Antenna using hybrid fractal slot for wideband applications," *Ain Shams Engineering Journal*, Vol. 9, no. 4, pp. 2491–2497, Dec. 2018. DOI: 10.1016/j.asej.2017.05.008.
[30] A. Shehni, J. Chakraborty, S. Sheikh, W. Kulesza, "Using Hilbert Curve Slot for Bandwidth Enhancement of Microstrip Patch Antenna," *HAL open Science*, IEEE-BTH Student Paper Contest 2011-12, IEEE Sweden Gwsac, Karlskrona, Sweden, pp.1-2, Jan.2012. DOI:10.5281/zenodo.3406144.
[31] A. Varshney, N. Cholake & V. Sharma, "Low-cost ELC UWB Fan-Shaped Antenna Using Parasitic SRR Triplet for ISM band and PCS Applications," *Inter J of Electr Letters*, Sept. 2021(Online). DOI: 10.1080/21681724.2021.1966655.
[32] A. Varshney, T. M. Neebha, V. Sharma, J. G. Jency & A. D. Andrushia, "Dodecagon-Shaped Frequency Reconfigurable Antenna Practically Loaded with 3-Delta Structures for ISM Band and Wireless Applications," *IETE Journal of Research*, Feb. 2022 (Online). DOI: 10.1080/03772063.2022.2034536.
[33] J.-M. Wierum, "Definition of a New Circular Space filling Curve," *Technical Report PC ,TR-001-02*, pp.01-12, March 2002.
[34] S. Killi, K.T.P.S Kumar, D. N. Kumar, S. Parasurampuram, "Design and Analysis of Pentagonal Patch Antenna with H-Tree Fractal Slots for S-Band and WI-Max Applications," *Inter J of Engg Sc and Computing*, Vol.6, no. 4, pp.4537-4540, April 2016. DOI: 10.4010/2016.1039.
[35] N. Kaur, J. S. Sivia, M. Kaur, "Design of Modified Sierpinski Gasket Fractal Antenna for C and X-Band Applications," *2015 IEEE 3rd International Conference on MOOCs, Innovation and Technology in Education (MITE)*, pp. 248-250, Oct. 2015. DOI: 10.1109/MITE.2015.7375324.
[36] J. Singh, N. Sharma, "A Design of Quad-Band Hexagonal Antenna with Fractal Slots using Inset Feeding Technique," *Inter J of Com App*, Vol.150, no. 8, pp.43-46, Sep. 2016. DOI: 10.5120/ijca2016911616.
[37] N. Kaur, S. Rani, "Analysis and design of rectangular patch Antenna with Triangular Fractal Techniques," *Inter J of Applied Sc & Tech*, Vol.6, no.2, March 2016.
[38] S. Kaur, J. S. Sivia, "Analysis and design rectangular patch with half rectangular fractal techniques," *Elsevier Inter Conf on Compu Modeling and Security*, Vol.85, pp.386-392, 2016. DOI: 10.1016/j.procs.2016.05.247.

Biography

N. M. MARY SINDHUJA received her BE degree in electronics and communication engineering from St Xaviers Catholic College of Engineering, Chunkankadai and ME degree in communication systems from Mepco Schlenk Engineering College, Sivakasi 2007 and 2009, respectively. She received her PhD degree from Anna University, Chennai during the year 2021 in the field of RF MEMS. Her research interests include design of microstrip antenna, analysis of RF MEMS components and design of phase shifters using space filling curve. She has published many book chapters, books, patent and research articles in several national and international journals and conferences. She is a lifetime member in IETE and ISTE.

ATUL VARSHNEY received his MTech in the microwave from MITS, Gwalior, India in 2008 and his BTech from UPTU, Lucknow in 2005. He is an RF microwave and antenna researcher and published 07 patents, many research articles, and books in this particular area. He has He also did a microstrip to waveguide transition project from ISRO-SAC, Ahmedabad. His research interests include design and fabrication, measurement and RLC electrical equivalent generation of

microstrip to waveguide transitions, ring resonators, microwave filters, planar antennas, metamaterial, and fractal structures, RLC Electrical Equivalent circuit's generation of any microwave 2D/3D components, frequency and pattern reconfigurable antennas, etc.